



¹Nuclear Science Division, Lawrence Berkeley National Lab; ²Department of Physics & Astronomy, University of Tennessee-Knoxville; ³Physics Division, Oak Ridge National Lab; ⁴Department of Physics, Florida Atlantic University; ⁵National Center for Computational Sciences, ORNL; ⁶Departments of Physics and Astronomy, University of California—Berkeley

Simulating Supernovae

The three “heads” of Chimera

- **Spectral neutrino transport**
MGFLD-TRANS in ray-by-ray approximation (Bruenn 1985)
- **Shock-capturing hydrodynamics**
Modified VH-1 (Blondin)
- **Nuclear kinetics**
XNet with 14-species α -network (Hix & Thielemann 1999)

Label	ZAMS Mass	# Particles	Elapsed Time (post-bounce)
B12-WH07	12 M_{\odot}	4000	1.410 sec
B15-WH07	15 M_{\odot}	5000	1.670 sec
B20-WH07	20 M_{\odot}	6000	1.692 sec
B25-WH07	25 M_{\odot}	8000	1.699 sec

Table 1. Models of Bruenn et al. (2016), initiated from stellar metallicity non-rotating progenitors from Woosley & Heger (2007)

Tracer Particle Method

A Lagrangian perspective

- Tracer particles record the temporal evolution of parcels of matter within the simulation.
- Thermodynamic and neutrino exposure histories facilitate post-processing calculations with larger nuclear networks.

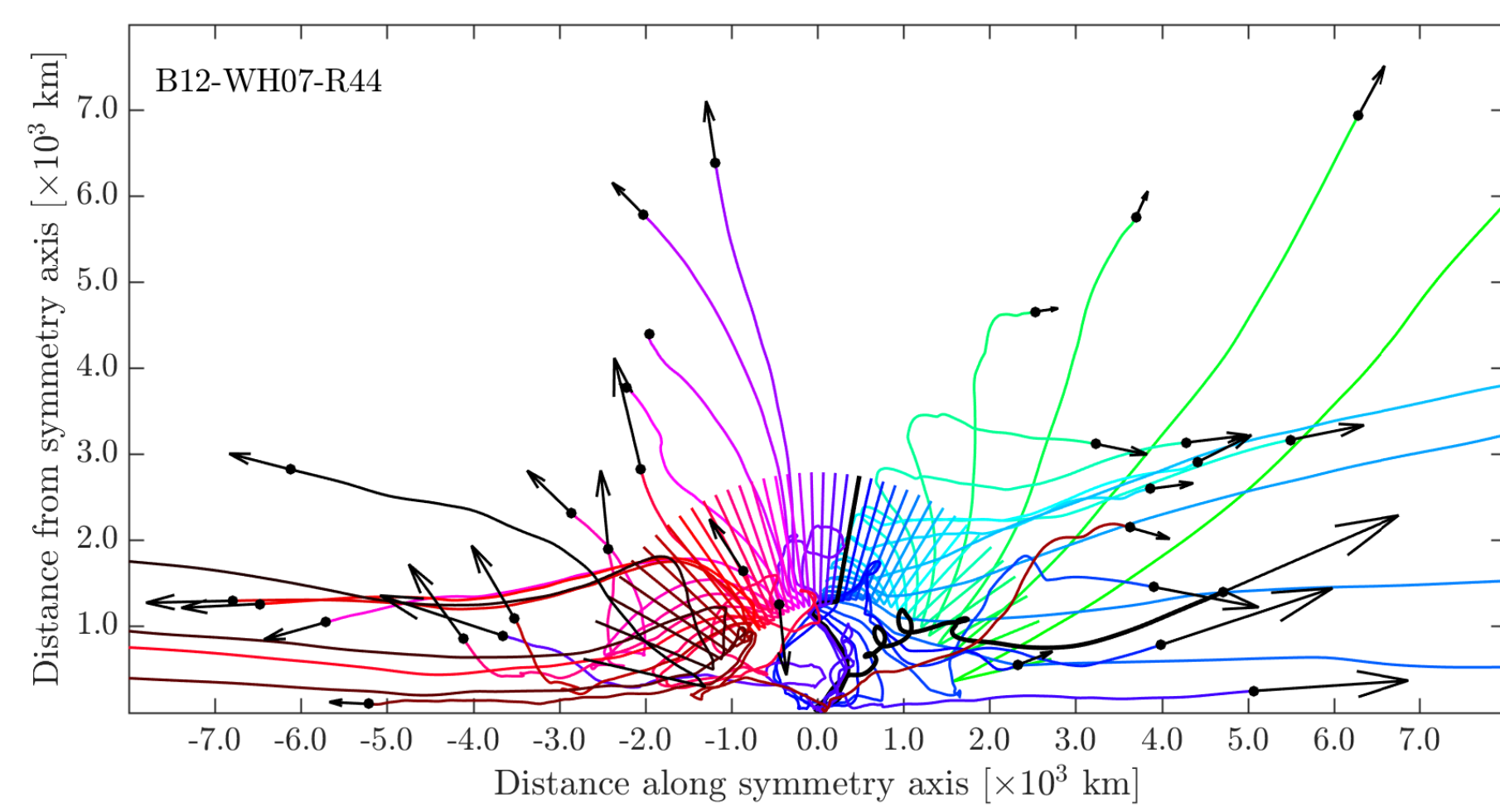


Figure 1. (above) Tracer particle trajectories from the same initial mass shell illustrate the complexity of a multi-dimensional “mass cut”.

Post-processing Methods

Parameterized thermodynamic trajectories

- TPM-generated thermodynamic profiles are extrapolated to the later times necessary to complete nuclear burning.
- Extrapolation assumes adiabatic expansion with timescale τ^* from the end of the simulation at time t_f to freeze-out conditions at time t_{fo} and a more slowly declining power-law trajectory for $t > t_{fo}$:

$$T(t) = \begin{cases} T_f \exp\left(-\frac{t-t_f}{3\tau^*}\right), & t_f < t \leq t_{fo} \\ T_f \exp\left(-\frac{t_{fo}-t_f}{3\tau^*}\right) \left(\frac{t}{t_{fo}}\right)^{-2/3}, & t > t_{fo} \end{cases}$$

$$\rho(t) = \begin{cases} \rho_f \exp\left(-\frac{t-t_f}{\tau^*}\right), & t_f < t \leq t_{fo} \\ \rho_f \exp\left(-\frac{t_{fo}-t_f}{3\tau^*}\right) \left(\frac{t}{t_{fo}}\right)^{-2}, & t > t_{fo} \end{cases}$$

- Neutrino-induced reactions assume constant T_ν and an integrated neutrino number flux $\phi_\nu \propto 1/r(t)^2$, where $r(t) = r(t_f) + v_r(t_f)\Delta t$ assumes a constant radial velocity.

References

- Bruenn, S. W. 1985, ApJS, 58, 771
 Bruenn, S.W., Lentz, E.J., Hix, W.R., et al. 2016, ApJ, 818, 123
 Fröhlich, C., Martínez-Pinedo, G., Liebendörfer, M., et al. 2006, Phys. Rev. Lett., 96, 142502
 Grefenstette, B.W., Harrison, F.A., Boggs, S.E., et al., Nature, 506, 339
 Hix, W. R. & Thielemann, F.-K. 1999, ApJ, 511, 862
 Wongwathanarat, A., Janka, H.-T., Müller, E., et al., 2016, arXiv e-prints, arXiv:1610.05643
 Woosley, S. E. & Heger, A. 2007, Phys. Rep., 442, 269

Comparisons to 1D Explosion Models

Nucleosynthetic yields

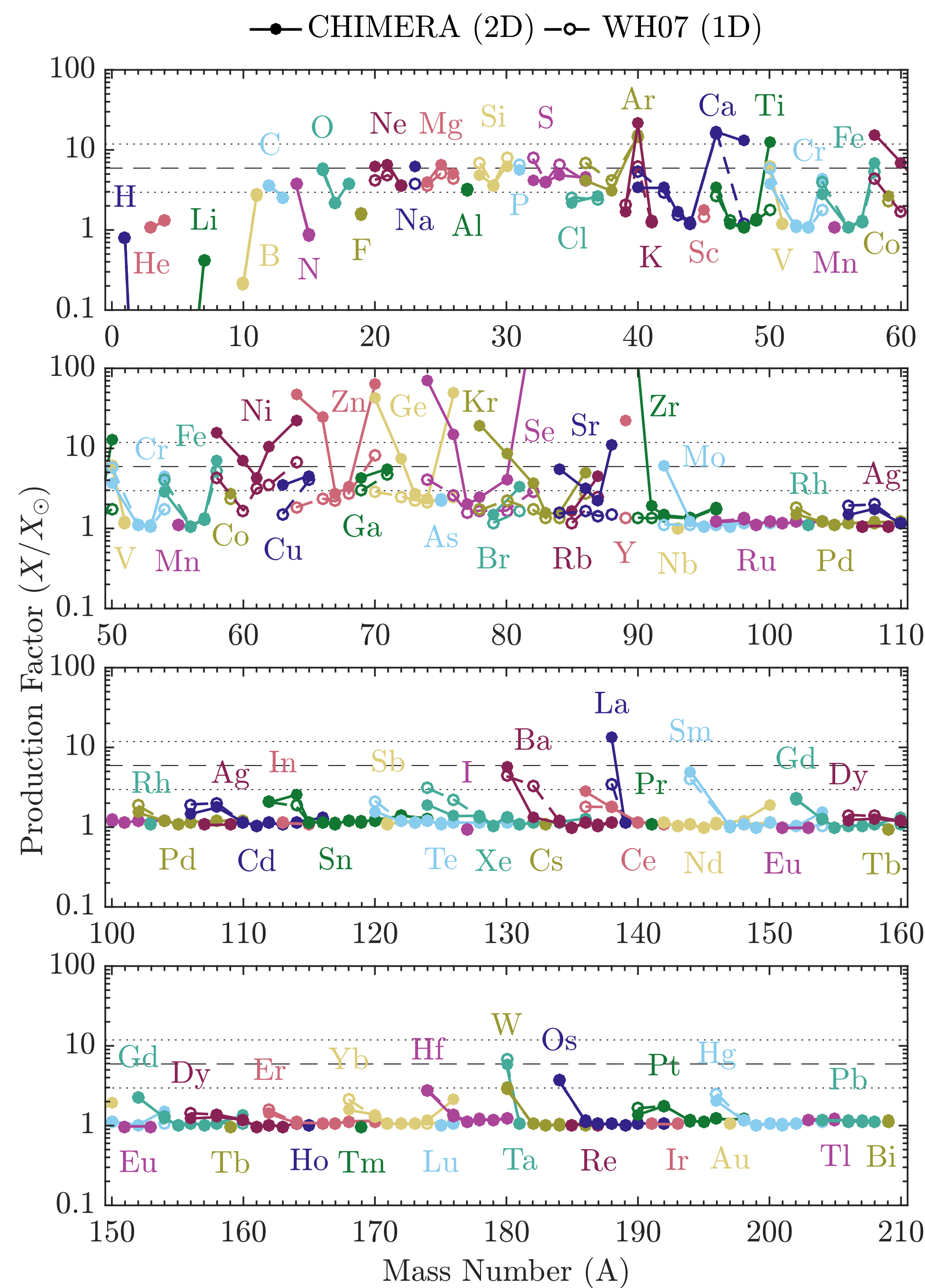


Figure 2. (above) Production factors at 100 s after bounce for B12-WH07 and the parameterized 1D explosion model of WH07. Normalization bands (dotted lines) are provided using a factor of two difference in the production factor of ^{16}O .

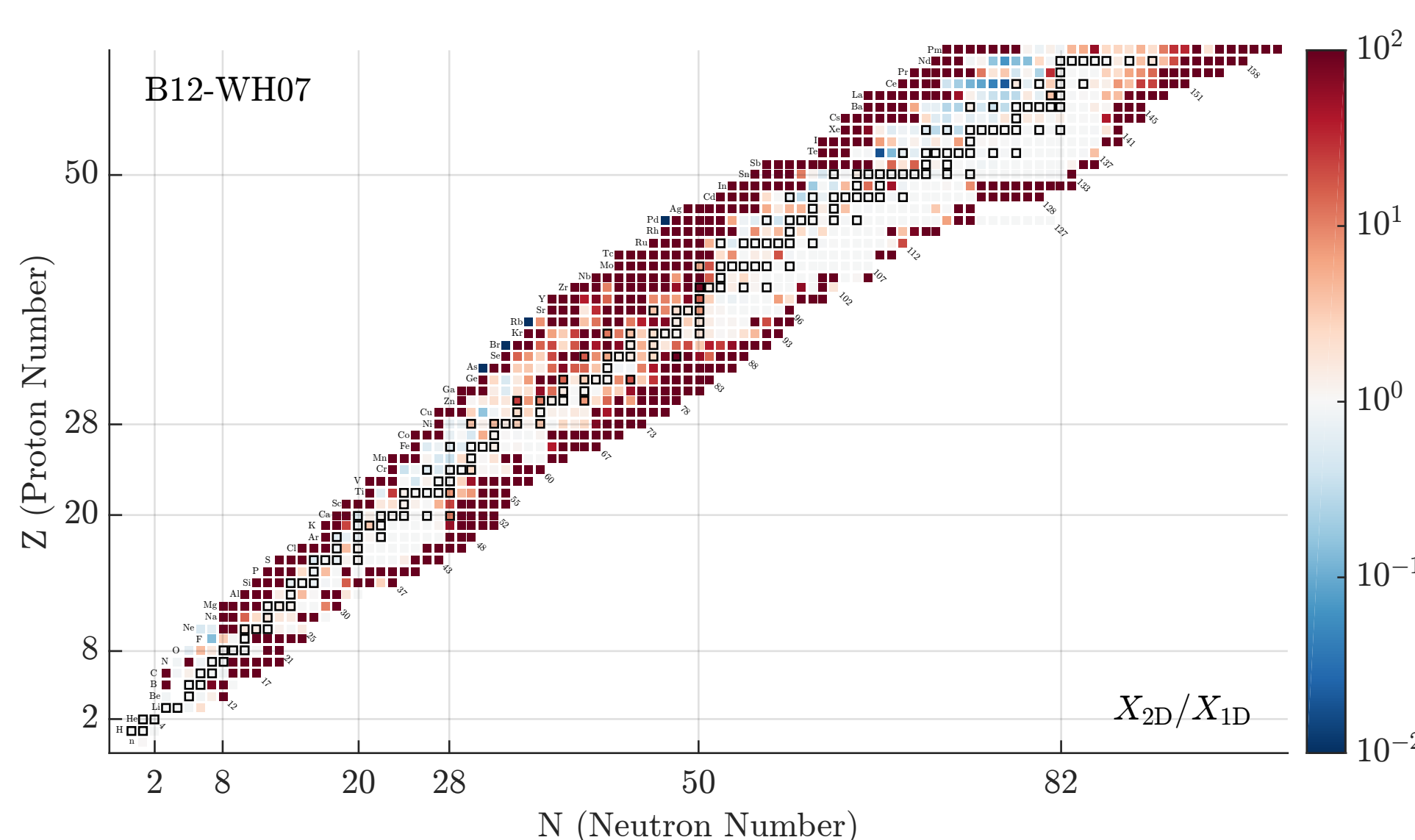


Figure 3. (above) Relative differences between a 2D Chimera model and its 1D WH07 counterpart at 100 s after bounce. B12-WH07 ejects an additional 0.027 M_{\odot} that is concentrated in proton-rich, intermediate-mass nuclei and various nuclei around $A = 90$.

A multi-dimensional “mass-cut”

- These differences are primarily attributed to continued accretion long after the launch of an explosion that serves to eject matter exposed to conditions unique to inner regions of shocked cavity that are not ejected in 1D simulations.

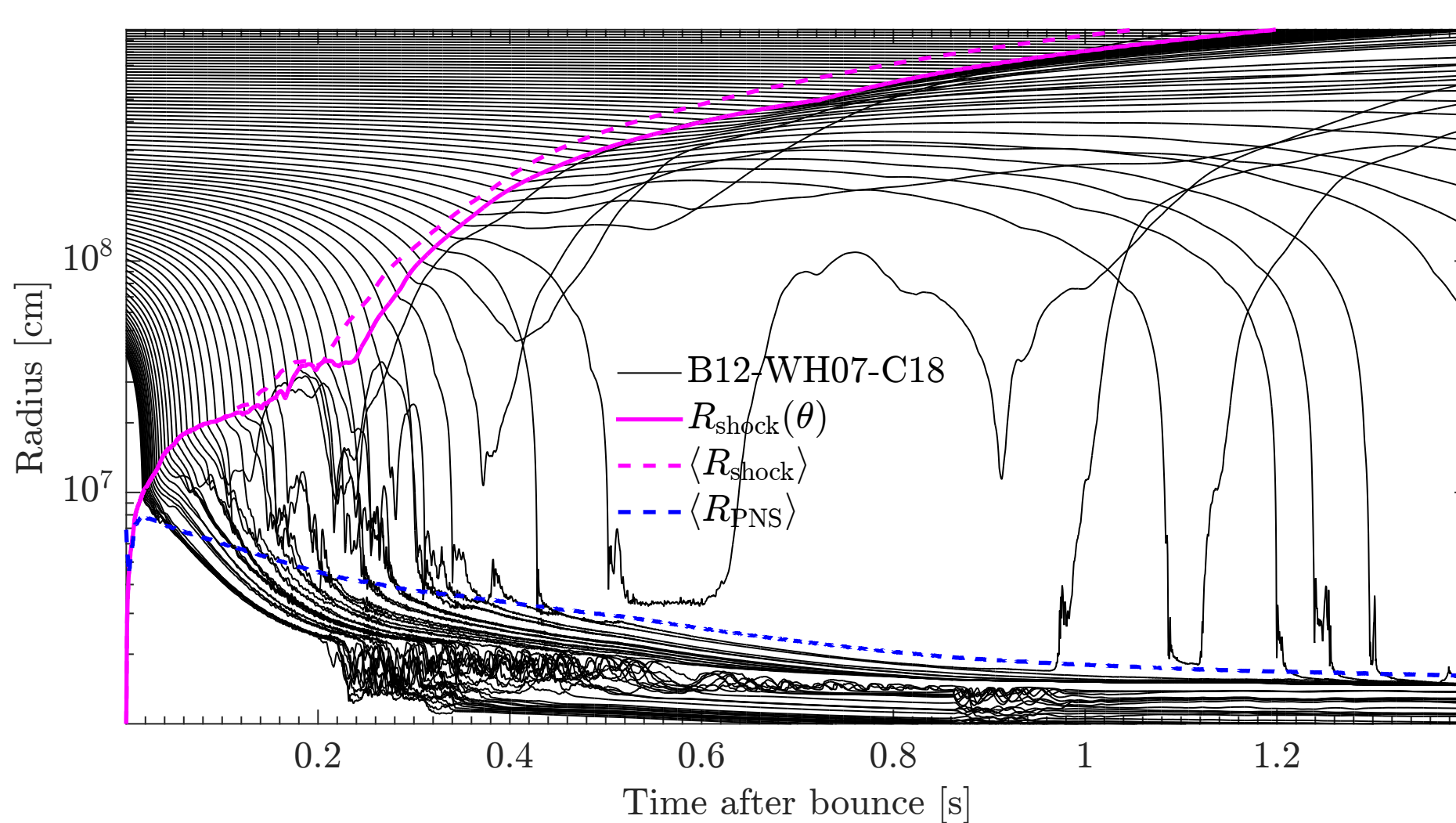


Figure 4. (above) Radial evolution of tracer particles in a column initially near the equatorial plane of the 12 M_{\odot} model, representing mass elements initially distributed in radius along $\theta = 82.8^\circ$. Lateral velocities behind the shock distort any prior resemblance to spherically symmetric models. The ejection of a tracer particle from the proto-NS at one second after bounce suggests a nascent neutrino-driven wind.

Comparisons to Observations

^{44}Ti and ^{56}Ni in supernova remnants

- The wealth of observational data for ^{44}Ti and ^{56}Ni makes the extent to which simulations can reproduce the total production and spatial distribution of these nuclei an excellent metric by which to gauge nucleosynthesis models.

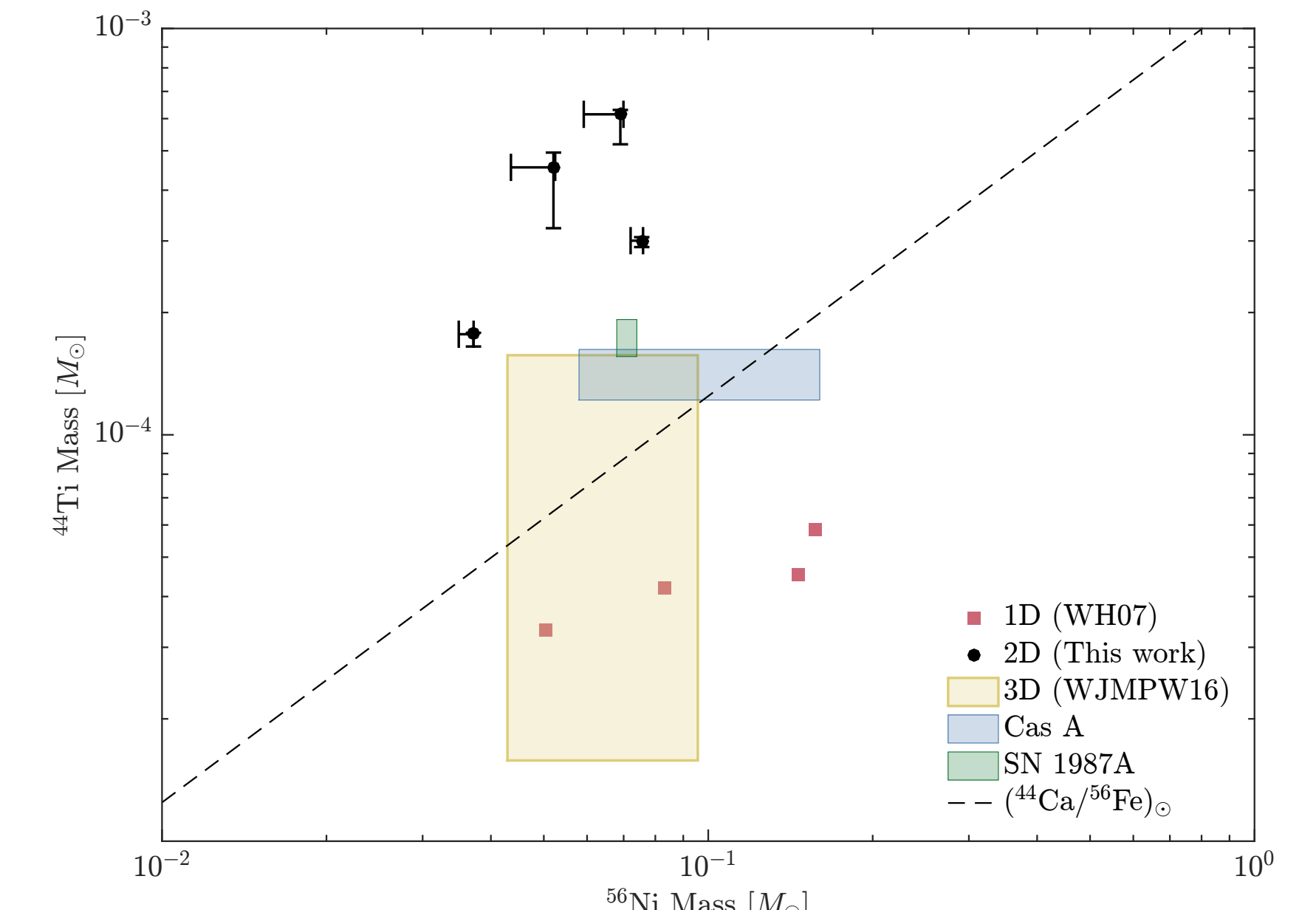


Figure 5. (above) Ejected ^{44}Ti and ^{56}Ni from this work compared with solar abundance ratio of radioactive decay products, SN remnant observations, and simulations from other groups. Error bars are dominated by uncertainty stemming from identification of the ejected matter.

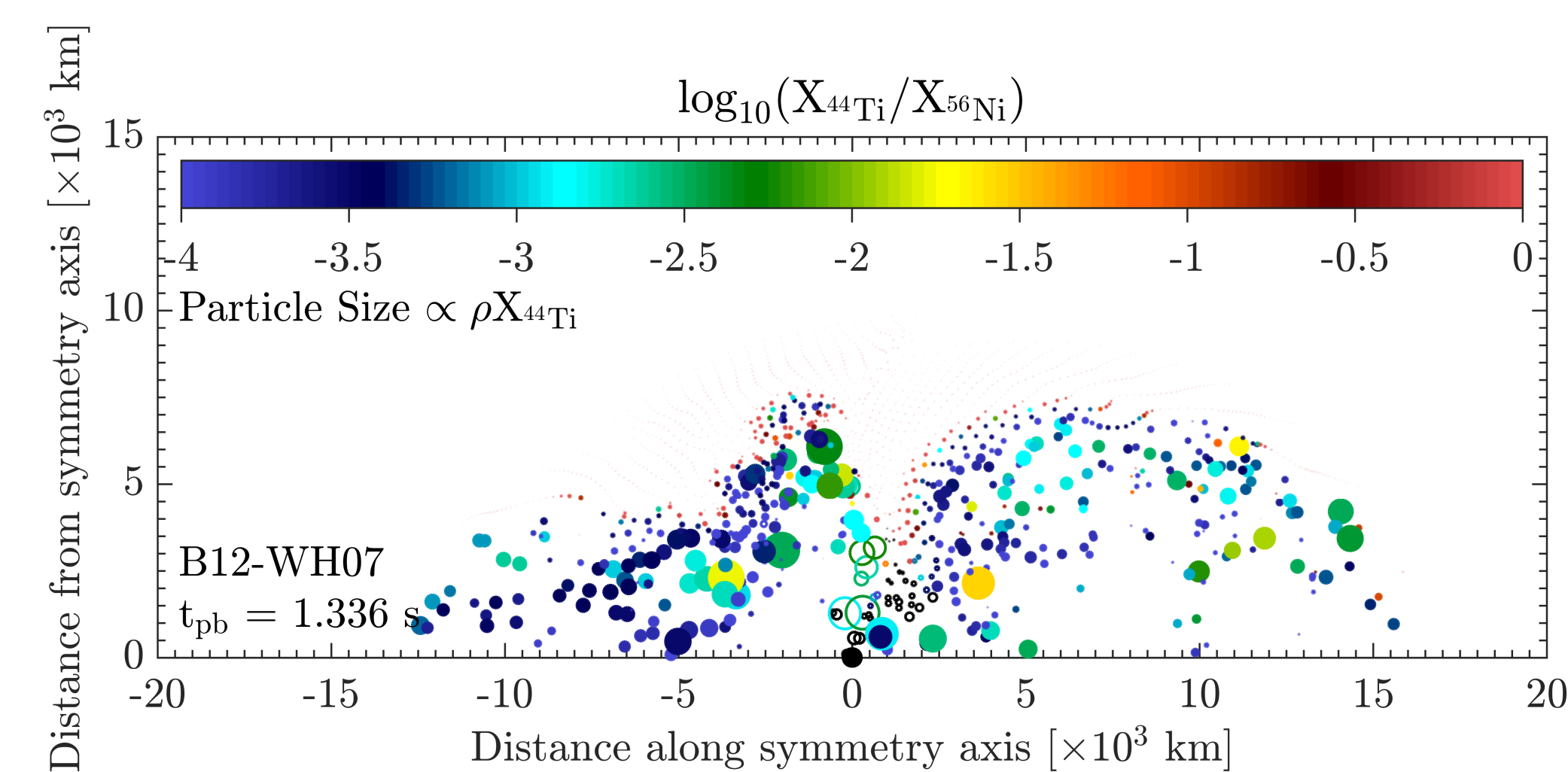


Figure 6. (above) Shocked tracer particles in B12-WH07 positioned at their positions at the end of the simulation and sized in proportion to the mass density of ^{44}Ti at one year after bounce. Ejected particles are colored by the mass fraction ratio of ^{44}Ti to ^{56}Ni . Large variations in this ratio suggest that the observed lack of correlation in Cassiopeia A (Grefenstette et al. 2014) may be a consequence of “hidden” iron that has yet to be heated by the reverse shock.

Conclusions

- First nucleosynthesis calculations from self-consistent, 2D CCSN simulations capturing the full development of an explosion with sophisticated neutrino transport
- Qualitative differences from parameterized 1D simulations of same initial models are largely attributed to thermodynamic histories unique to multi-D explosions.
- Overproduction of n-rich isotopes ^{48}Ca , ^{50}Ti , ^{54}Cr , ^{58}Fe , ^{64}Ni , ^{70}Zn , ^{76}Ge , and ^{82}Se relative to 1D models could address a long-standing mystery of astrophysical origins.
- Significant increase in production of several p-nuclei (e.g. ^{88}Sr , ^{90}Zr , ^{92}Mo , ...) consistently underproduced by parameterized 1D models, hinting at a *lighter element primary process* (LEPP)
- ^{44}Ti and ^{56}Ni are slightly overproduced in 2D relative to observations of SN 1987A and Cassiopeia A, as well as recent 3D simulations by Wongwathanarat et al. (2016).
- Highly asymmetric ^{44}Ti distribution correlated with ^{56}Ni , but $^{44}\text{Ti}/^{56}\text{Ni}$ ratio can vary by several orders of magnitude.

Acknowledgements

The research presented here was supported by the U.S. DOE Offices of Nuclear Physics and Advanced Scientific Computing Research and the NASA Astrophysics Theory and Fundamental Physics Program (grants NNN08AH711 and NNN11AQ721). Simulations were performed via NSF TeraGrid resources provided by the National Institute for Computational Sciences (grant TG-MCA08X010); resources of the National Energy Research Scientific Computing Center, supported by the U.S. DOE Office of Science under Contract No. DE-AC02-05CH11231; and at the Oak Ridge Leadership Computing Facility, supported by the U.S. DOE Office of Science under Contract No. DE-AC05-00OR22725.